Magnetic Resonance Imaging 61 (2019) 260–266

Contents lists available at ScienceDirect

Magnetic Resonance Imaging

journal homepage: www.elsevier.com/locate/mri

Original contribution

Evaluating a novel free-breathing accelerated cardiac MRI cine sequence in patients with cardiomyopathy☆

Idan Roifman[a,b,c,*], Jose Gutierrez[a], Edison Wang[a], Labonny Biswas[a], John Sparkes[a], Kim A. Connelly[a,d], Graham A. Wright[a,b,c]

[a] Sunnybrook Health Sciences Center, University of Toronto, Toronto, Canada
[b] Institute of Health Policy Management and Evaluation, University of Toronto, Toronto, Canada
[c] Institute for Clinical Evaluative Sciences, University of Toronto, Toronto, Canada
[d] St. Michael's Hospital, University of Toronto, Toronto, Canada

ARTICLE INFO

Keywords:
Accelerated magnetic resonance imaging
Cardiomyopathy
Free-breathing cine imaging

ABSTRACT

Introduction: Cardiac magnetic resonance imaging (CMR) is the gold standard for the assessment of left ventricular (LV) function. However, traditional sequences are time-consuming and require breath-holding. Our aim was to evaluate the image quality of LV functional assessment with a novel, accelerated, free-breathing cine sequence and to compare LV functional parameters between it and a traditional sequence.

Methods: This was a prospective cohort study of 31 patients with cardiomyopathy. All studies were performed on a 1.5 Tesla scanner. LV function was first determined using contiguous short axis slices covering the left ventricle from the base to the apex acquired with the standard cine sequence. Next, the accelerated sequence was acquired for each patient. The Wilcoxon Matched-Pair Sign Rank Test was used to compare image quality between the accelerated and traditional cine imaging sequences. Standard and accelerated left ventricular volumes and ejection fraction were compared using linear regression. Bland-Altman plots were then constructed to evaluate agreement, interobserver and intraobserver variability for left ventricular volumes and ejection fraction.

Results: Mean acquisition time was 29 s for the accelerated sequence vs. 410 s for the traditional sequence. Qualitative assessment of image quality was similar for both sequences ($p = 0.23$). There were no significant differences in terms of LVEDV, LVESV, LVSV, LV mass and LVEF when calculated from either sequence with very good agreement between the standard and accelerated sequences. The mean differences with 95% limits of agreement were as follows: LV mass (−0.6, −22.9 g, 21.6 g), LVEDV (5.1 mL, −18.4 mL, 28.9 mL), LVEF (−0.3, −5.4, 4.7), LVESV (4.0 mL, −12.0 mL, 20.0 mL), LVSV (1.1 mL, −13.3 mL, 15.5 mL). Interobserver variability ranged from 0.1 to 6.3% while intraobserver variability ranged from 0.1 to 1.8%.

Conclusions: The accelerated free-breathing cine sequence performed similarly to standard of care multi breath-hold cine imaging and was acquired in a fraction of the time without the need for breath-holding. If applied to clinical practice, this sequence can significantly reduce scanning time and facilitate CMR scanning in those patients who are unable to breath-hold.

Abbreviations: CI, confidence interval; CMR, cardiovascular magnetic resonance; EDV, end-diastolic volume; EF, ejection fraction; ESV, end-systolic volume; LV, left ventricle; SD, standard deviation; SV, stroke volume

☆ Acknowledgements: None.

Funding sources: Dr. KA Connelly is supported by a New Investigator Award from the Canadian Institutes of Health Research and an Early Researcher Award from the Ministry of Ontario. Dr. Idan Roifman is supported by National New Investigator and Ontario Clinician Scientist Awards from the Heart and Stroke Foundation of Canada. Dr. Graham Wright is supported by a Tier 1 Canada Research Chair in Imaging for Cardiovascular Interventions. This research is supported by an operating grant from the Federal Development Agency of Canada and a matching financial contribution from HeartVista Inc. HeartVista Inc. provided a prototype version of their accelerated cine sequence for our evaluation. The funding bodies had no role in the design of the study and collection, analysis and interpretation of data and in writing the manuscript.

* Corresponding author at: Sunnybrook Health Sciences Centre, University of Toronto, Adjunct Scientist, ICES, 2075 Bayview Avenue, Toronto, On M4N-3M5, Canada.

E-mail address: idan.roifman@sunnybrook.ca (I. Roifman).

https://doi.org/10.1016/j.mri.2019.06.008
Received 2 April 2019; Received in revised form 5 June 2019; Accepted 7 June 2019

1. Introduction

Evaluation of left ventricular function is one of the most common indications for cardiovascular magnetic resonance (CMR) imaging [1,2]. In many disease states, such as cardiomyopathy, CMR-determined left ventricular function, and most prominently left ventricular ejection fraction (LVEF), has been independently linked with prognosis [3–5]. The current standard of care sequence to determine LVEF is multiple breath-hold steady state free precession (SSFP) cine imaging with one myocardial slice acquired per breath-hold. While this method is accurate and reproducible, it is also time consuming, taking approximately 6–8 min to acquire images [6–8]. The long cine acquisition time is a significant contributor for prolonged overall CMR scan times, in turn leading to barriers in CMR availability and long wait times in many jurisdictions [9,10]. Further, many patients are unable to perform the multiple breath-holds that are required to produce diagnostic images with traditional cine CMR imaging.

In order to address these issues, a novel, free-breathing, real-time, accelerated cine SSFP (accelerated SSFP) sequence has recently been developed. This sequence was developed to accelerate current imaging times and reduce the need for breath-holding. However, the accuracy of left ventricular function assessment by this new technology is currently unknown. The goal of this study was to compare important metrics of left ventricular function (left ventricular ejection fraction, volumes and mass) between the novel accelerated and gold standard, multiple breath-hold SSFP cine sequences. We hypothesized that there would be no significant difference in the assessment of these parameters between the two sequences and that intra and interobserver agreement for the novel sequence would be high.

2. Materials and methods

2.1. Study population

This was a single site prospective cohort study that enrolled patients who were referred for CMR for the indication of cardiomyopathy from September 2013–December 2016. We enrolled patients referred with cardiomyopathy because the main goal of this study was to evaluate LV function with the novel accelerated cine sequence. In the assessment of LV function in such patients, it is important to quantify LVEF in order to help inform who will receive evidence-based medications and implantable devices such as an implantable cardioverter defibrillators. As such, the patient population referred for cardiomyopathy, most with abnormal LV function, was considered to be the optimal patient population for this evaluation. All patients underwent standard cine SSFP imaging, which served as the standard of reference, and the accelerated cine imaging sequence. Exclusion criteria included presence of hemodynamic instability, pregnancy and failure to provide informed consent to participate in the study.

2.2. CMR protocol

All studies were performed on a GE Optima 1.5 Tesla MR scanner with a 32-channel coil (GE Healthcare, Waukesha, WI). LV function was first determined using contiguous short axis slices covering the left ventricle from the base to the apex acquired with the standard SSFP sequence. Next, the accelerated sequence was acquired for each patient. The accelerated sequence utilized a 36-interleave variable-density spiral acquisition and fully refocused gradient moments to establish steady-state free precession (SSFP) contrast (HeartVista Inc., Menlo Park, CA). Two cardiac cycles were acquired per slice location, using prospective cardiac triggering to advance the slice acquisition. Slices were acquired progressively from base to apex to minimize the slice-to-slice impact of respiratory motion. Within each slice location, interleaves were continuously acquired over the two heartbeats and retrospective resampling was used for image reconstruction.

Table 1
Technical parameters of the traditional and accelerated cine sequences.

	Traditional cine	Accelerated cine
Technical sequence description	Multi-slice steady-state free precession	Spiral acquisition steady-state free precession
Parallel imaging	No	Yes, approximately 2×
Receiver coil	32-Channel	32-Channel
Breath-hold	Yes	No
Mean acquisition time (s)	416	29
TR	5	4
Mean field of view (mm)	357 × 357	339 × 339
Flip angle (°)	56	59
Cardiac phases	20	40
Mean number of slices	15	15
Slice thickness (mm)	8	8
In-plane spatial resolution (mm)	1.4 × 1.4	2.5 × 2.5
Temporal resolution (ms)	46	73

Table 2
Characteristics of the patient population.

N	31
Age (years)	62.3 ± 8.6
Sex (male)	26 (84%)
Active smoking	8 (26%)
Diabetes	10 (31%)
Hypertension	14 (45%)
Dyslipidemia	8 (26%)
Coronary artery disease	18 (58%)
Cerebrovascular disease	3 (10%)
Valvular disease	2 (6%)
Atrial fibrillation	1 (3%)

Partially parallel imaging with localized sensitivities (PILS) parallel acceleration [11] and variable-density spiral acquisition were both utilized to produce an acceleration factor of approximately 2-fold. The entire dataset for each image was acquired in a free-breathing, real-time fashion rather than being segmented over several heartbeats. Specific CMR parameters for both sequences are summarized in Table 1.

2.3. Image analysis

Image analysis was performed via CVI-42 version 4.1.8 software (Circle Cardiovascular Imaging, Calgary, Alberta, Canada). One radiologist and one cardiologist, both of whom were certified as level 3 trained by the Society for Cardiovascular Magnetic Resonance, independently evaluated all the images.

2.4. Qualitative analysis

The image quality of each image was evaluated visually and scored on a five-point scale as has been previously described:

1 = non-diagnostic image quality (extensive artifact affecting volumetric analysis), 2 = poor image quality (moderate artifact affecting volumetric analysis), 3 = adequate quality, mild artifact affecting volumetric analysis, 4 = good quality minimal artifact affecting volumetric analysis, and 5 = excellent quality, no artifact [12].

2.5. Quantitative analysis

The endocardium and epicardium of the left ventricle were manually and independently contoured at end-systole and end-diastole by both image evaluators in order to calculate mass, volumes and ejection fraction. The most recent SCMR guideline was the standard utilized for contouring [13]. Papillary muscles and endocardial trabeculations were included in LV cavity volumes in a manner previously described [12,14–17].

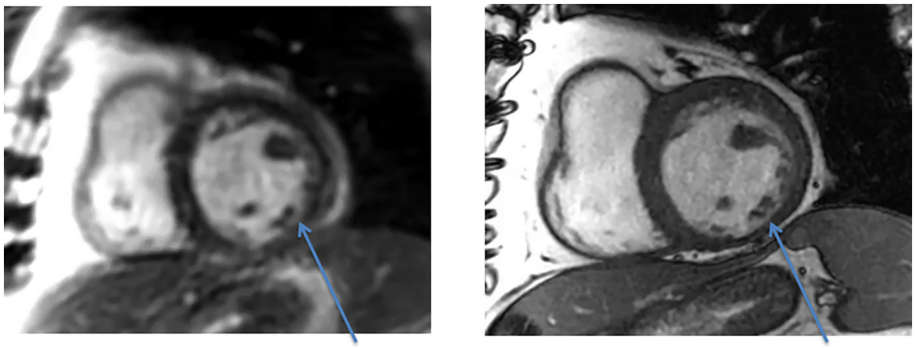

Fig. 1. Comparison of the accelerated and traditional cine sequences in a mid-ventricular myocardial slice in a patient post inferior/inferolateral myocardial infarction. The blue arrows denote the location of myocardial thinning and hypokinesis. Please also see accompanying Videos 1 and 2 in the Supplemental materials. (For interpretation of the references to color in this figure legend, the reader is referred to the web version of this article.)

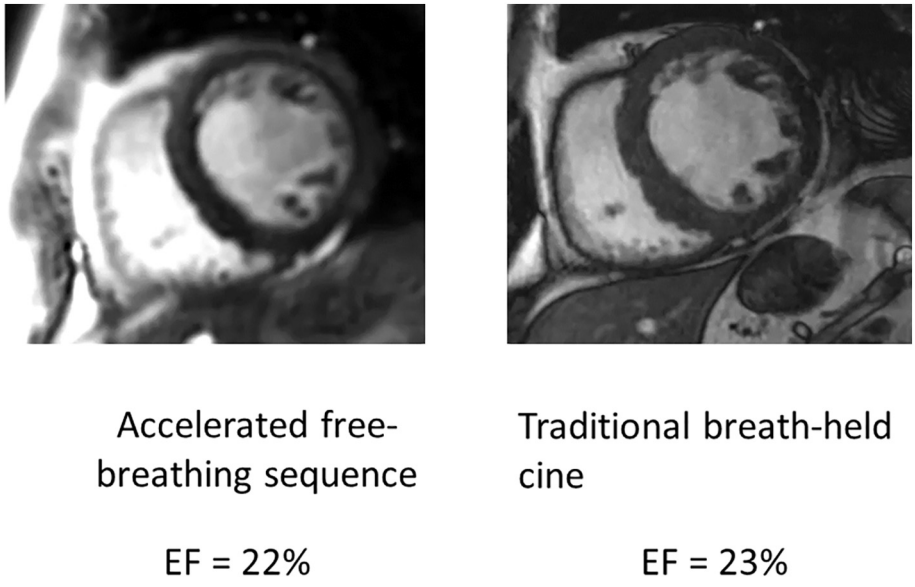

Fig. 2. Comparison of the accelerated and traditional cine sequences in a mid-ventricular myocardial slice in a patient with global hypokinesis with regional variability as a result of non-ischemic dilated cardiomyopathy. LVEF was calculated and presented for both sequences. Please also see accompanying Videos 3 and 4 in the Supplemental materials.

Table 3
Left Ventricular measurements for traditional cine CMR vs. accelerated cine CMR.

Parameter	Standard cine	Accelerated cine	p(Diff)
	(Mean ± SD)	(Mean ± SD)	Mann-Whitney test
LVEDV (mL)	212.5 ± 85.4	207.4 ± 84.1	0.75
LVESV (mL)	142.4 ± 77.4	138.4 ± 75.8	0.76
LVSV (mL)	70.1 ± 19.3	69.0 ± 19.2	0.71
LV mass (g)	150.3 ± 48.5	150.9 ± 50.2	0.99
LVEF (%)	36.3 ± 12.7	36.6 ± 12.7	0.91

Abbreviations: LVEDV: left ventricular end diastolic volume, LVESV: left ventricular end-systolic volume, LVSV: Left ventricular stroke volume, LVEF: left ventricular ejection fraction, mL: milliliter, g: gram.

2.6. Statistical analysis

Continuous variables were reported as mean ± standard deviation and categorical variables as proportions. The Wilcoxon Matched-Pair Sign Rank Test was used to compare image quality between the accelerated and traditional cine imaging sequences. Standard and accelerated left ventricular parameters (LV mass, LV end diastolic volume (LVEDV), LV end systolic volume (LVESV), LV stroke volume (LVSV) and LV ejection fraction (LVEF)) were compared using linear regression. Bland-Altman plots were constructed to evaluate agreement, interobserver and intraobserver variability of each parameter. A p-value of < 0.05 was considered statistically significant. All statistical analyses were performed using SAS version 9.3 (Cary, North Carolina). This study was approved by the research ethics board at our institution.

3. Results

3.1. Patient characteristics

31 patients were enrolled in this study. Table 2 summarizes the characteristics of the patient population. The mean age was 62.3 ± 8.6 years. 84% of the patients were male. 26% of the patients were active smokers, 31% had diabetes, 45% had hypertension and 26% had dyslipidemia. 58% of the patients had a documented history of obstructive CAD (ischemic cardiomyopathy) while only 2 patients (6%) had significant (more than mild) valvular disease. One of the 31 patients (3%) had atrial fibrillation. Mean acquisition time was 410 s for the traditional cine sequence and 29 s for the accelerated cine sequence.

3.2. Image quality

Figs. 1 and 2 show still frames of cines from representative slices of both standard cine CMR and accelerated sequences from two patients

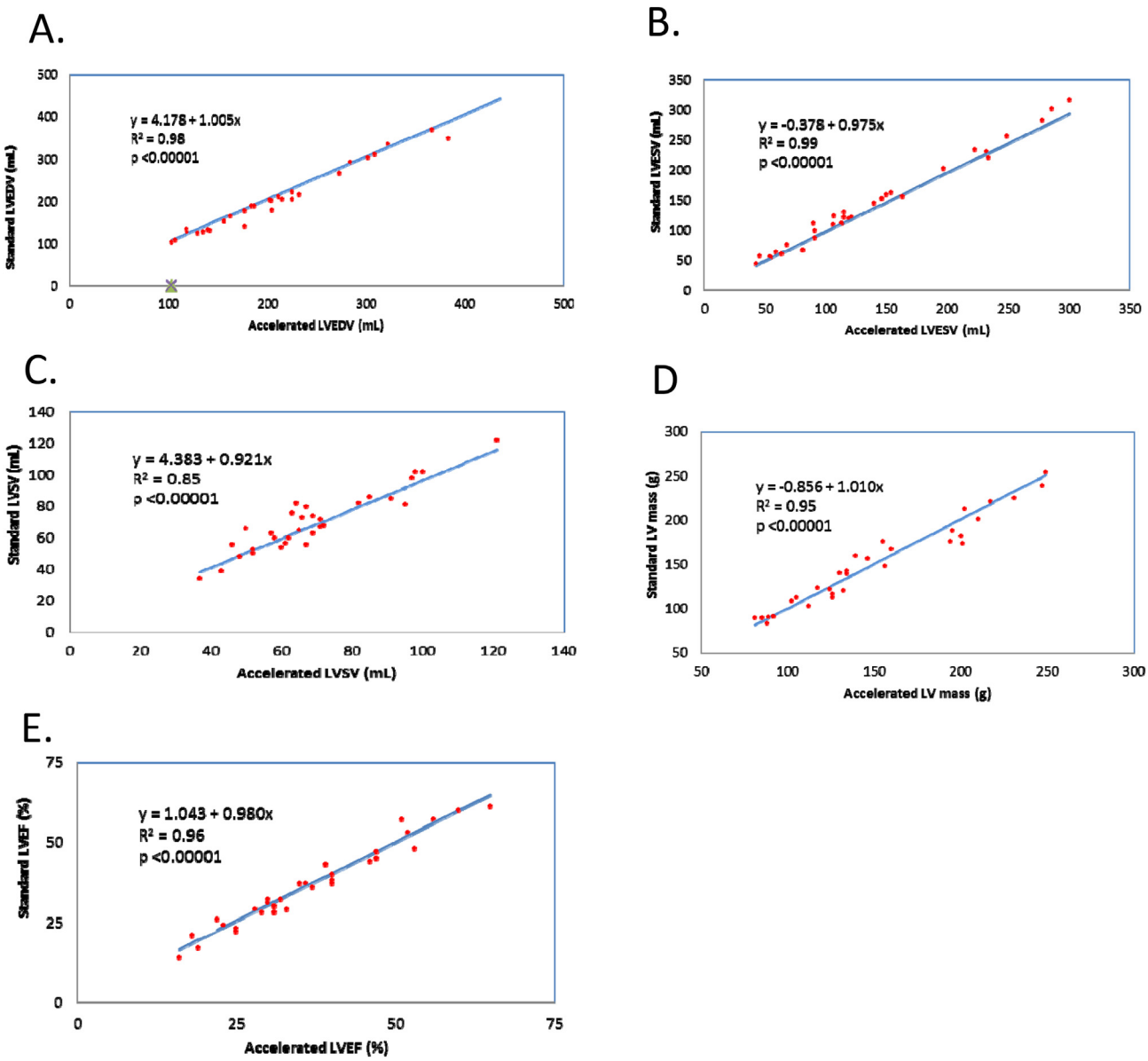

Fig. 3. Scatterplots comparing (a) LVEDV, (b) LVESV, (c) LVSV, (d) LV mass and (e) LVEF between the traditional and accelerated cine sequences.

who were enrolled in our study, one with ischemic cardiomyopathy and the other with non-ischemic cardiomyopathy (corresponding videos are provided in the Supplemental materials). Images from both cine CMR sequences were rated in the very good to excellent diagnostic range. Image quality for the accelerated sequences was ranked slightly lower when compared to the traditional cine sequences (4.5 vs. 4.7 respectively) although this difference did not meet statistical significance ($p = 0.23$).

3.3. Left ventricular function

Mean LV function for the entire cohort was moderately reduced, with an LVEF of approximately 36%. There were no significant differences in terms of LVEDV, LVESV, LVSV, LV mass and LVEF when calculated by either sequence (see Table 3).

Fig. 3 displays the results of the regression analyses comparing the traditional vs. accelerated sequences with regard to LVSV, LV mass, LVEF, LVEDV and LVESV. The linear regression models show very good agreement between the standard and accelerated sequences with regard to these parameters. Bland-Altman analyses for all parameters were performed and are visually displayed in Fig. 4. The mean differences with 95% limits of agreement were as follows: LV mass (−0.6, −22.9 g, 21.6 g), LVEDV (5.1 mL, −18.4 mL, 28.9 mL), LVEF (−0.3, −5.4, 4.7), LVESV (4.0 mL, −12.0 mL, 20.0 mL), LVSV (1.1 mL, −13.3 mL, 15.5 mL). Inter and intraobserver variability for all LV functional parameters are reported in Table 4. Interobserver variability ranged from 0.1 to 6.3% while intraobserver variability ranged from 0.1 to 1.8%.

4. Discussion

We found that there was very good to excellent image quality for both the accelerated cine imaging and standard of care cine imaging. The accelerated sequence produced images in approximately 29 s vs. approximately 6–7 min for the traditional sequence. There were no significant differences in terms of left ventricular mass, volumes and ejection fraction between the accelerated and traditional techniques, with no clinically significant bias and with good intra and interobserver agreement.

Cardiac magnetic resonance (CMR) cine imaging is the core pillar in

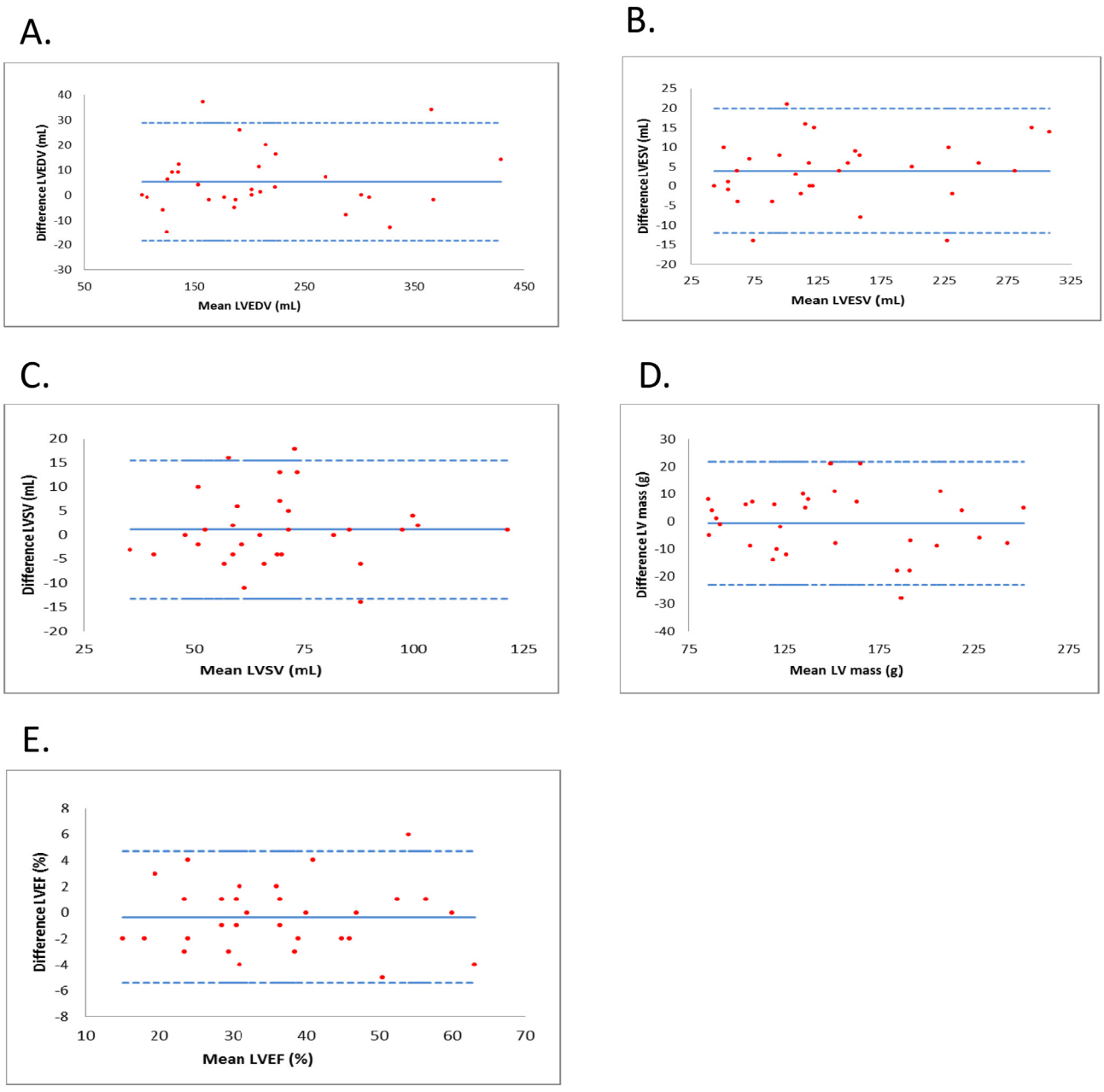

Fig. 4. Bland-Altman plots demonstrating the mean difference and 95% limits of agreement between the traditional and accelerated sequences for (a) LVEDV, (b) LVESV, (c) LVSV, (d) LV mass and (e) LVEF.

the assessment of patients with cardiomyopathy, the number one indication for CMR worldwide [18–20]. Cine imaging allows for accurate assessment of left ventricular volumes and ejection fraction (LVEF) [8,21–25]. LVEF is used to risk stratify patients and to direct management that has been shown to improve patient outcomes [4,26,27]. Despite its importance there has been a lack of uptake of CMR, most notably in North America. For example, recent data from Canada indicate that there are long wait-lists for this important diagnostic test, regularly exceeding 9–12 months in many institutions. This lack of availability results in delays in patient management. One reason for the long-wait times is the long acquisition times for currently used CMR clinical protocols [10]. Traditional cine imaging utilizes electrocardiogram-gating and breath-holding. Imaging datasets are acquired over multiple breath-holds and then combined to produce the final images. Typically, 1–2 myocardial slices are acquired with each breath-hold. Covering the entire left ventricle requires approximately 6–10 breath-holds and 6–8 min of scan time [2,7]. The long wait times have provided an impetus to develop faster imaging protocols. Recently, Siemens Inc. has developed compressed sensing cine CMR where images are acquired over a single-breath hold. A recent paper reported that LV functional assessment by this technique was similar to traditional cine imaging [12]. Similarly, our data indicate that the accelerated cine technique that we evaluated produced similar assessments of left ventricular structure and function but in a fraction of the time. The R^2 values, mean differences and inter and intraobserver variability measures that we reported were similar to those reported by others evaluating novel cine imaging techniques [12,28–30]. In addition, the technique we evaluated utilized a free-breathing, real-time approach to image acquisition. The advantage of this technique is two-fold. First, by not requiring breath-holding one is able to acquire images in a more rapid manner. Second, the technology potentially expands the pool of patients who would be able to undergo cine CMR, including

Table 4
Intra-observer and inter-observer variability of accelerated cine CMR.

Parameter	Difference	Variability (%)	R^2	Slope	p-Value
	(Mean ± SD)	(Mean ± SD)[a]			
Intra-observer					
LVEDV (mL)	0.3 ± 1.4	0.6 ± 0.6	1.00	0.99	< 0.0001
LVESV (mL)	0.6 ± 2.5	1.9 ± 1.3	1.00	1.00	< 0.0001
LVSV (mL)	−0.3 ± 3.1	3.7 ± 3.8	0.97	1.00	< 0.0001
LV mass (g)	1.8 ± 11.6	6.5 ± 4.8	0.94	1.01	< 0.0001
LVEF (%)	0.1 ± 1.0	3.0 ± 2.5	0.99	0.97	< 0.0001
Inter-observer					
LVEDV (mL)	6.3 ± 11.6	3.1 ± 5.1	0.98	1.00	< 0.0001
LVESV (mL)	4.0 ± 7.2	2.9 ± 4.3	0.99	1.01	< 0.0001
LVSV (mL)	2.1 ± 6.1	4.8 ± 7.8	0.90	0.97	< 0.0001
LV mass (g)	0.1 ± 12.4	7.2 ± 4.2	0.93	0.96	< 0.0001
LVEF (%)	3.2 ± 1.7	2.9 ± 4.3	0.98	1.00	< 0.0001

[a] Variability (%) assessed by Bland-Altman (absolute difference between methods divided by the mean of the two methods).

those who are unable to breath-hold and those with cardiac arrhythmias such as atrial fibrillation. The potential advantage of this sequence in patients with arrhythmias can be summarized as follows: In traditional cine imaging, each image is acquired over multiple heart beats. In that case, high-quality images require that the heart return to exactly the same location at each heartbeat. This can be problematic in the case of arrhythmias leading to significant motion artifact. In contrast, the novel accelerated sequence that we tested utilizes cardiac gating to advance the slice position. After advancement, two heartbeats of data are acquired for each position. After two heartbeats the sequence advances to the next location. At each slice location, data are acquired continuously in a real-time fashion without any assumptions or segmentation based upon the cardiac cycle. If an arrhythmia occurs during the acquisition of any slice, high-quality images will be obtained of that arrhythmic heart-beat.

A major drawback to the radial cine acquisition employed in the novel accelerated cine sequence that we evaluated lies in its sensitivity to off-resonance artifacts caused by the main field inhomogeneity [31]. This characteristic can lead to artifacts from implanted materials such as sternal wires which can ultimately culminate in distorted image quality. There are several corrections performed on the novel accelerated sequence to minimize off-resonance artifacts for spiral images. First, independent shims are applied for each slice, optimizing the field correction for each slice individually. Second, the sequence utilizes very short spiral interleaves. Because these artifacts arise from spin dephasing during the acquisition window, shorter acquisitions limit signal loss. These corrections significantly minimize image blurriness such that the artifact does not extend into the myocardium where it can impact myocardial contouring, and subsequently, calculation of ventricular volumes and ejection fraction. This technology contrasts with compressed sensing which uses spatiotemporal regularization, incorporating the assumption that the acquired data is sparse in the wavelet domain. When pushed to high acceleration factors, this regularization can lead to significant artifact and image blurring which often also extends into the myocardium.

In our study, we had two subjects with in-situ sternal wires as the result of prior cardiac surgery. The videos and still frames of one of these subjects are provided in Videos 1 and 2 and in Fig. 1. As can be appreciated, the artifact from the sternal wires is more pronounced in the radial acquisition when compared to the traditional cartesian SSFP acquisition. However, the artifact does not extend into the epicardium and endocardium of the heart and thus did not influence subsequent calculation of LV mass, volumes and EF.

4.1. Clinical importance

Our work is the first step towards clinical validation of a novel, accelerated free breathing cine CMR technique in a population of patients with cardiomyopathy utilizing a standard SSFP sequence as the gold standard. If our results are replicated in larger multi-centre studies, this sequence may replace traditional and slow cine imaging techniques, thus allowing for more scans to be performed per unit time and contributing to the reduction in wait times for CMR. Further, this technique can potentially expand the pool of patients who would be eligible to undergo CMR by introducing the possibility of accurate scanning for those who are unable to hold their breath and those with arrhythmias such as atrial fibrillation.

4.2. Limitations

Our study must be interpreted in the context of its limitations. First, this is a relatively small, single-centre study. With that said, it is similar in size to a number of previously published studies evaluating new MRI sequences [28,29,32,33]. Future, larger, multi-centre studies will need to be conducted in order to confirm our results. Second, a potential application of this free-breathing technique lies in patients with cardiac arrhythmias. In our cohort, only one of our patients had atrial fibrillation at the time of the scan. Future studies aimed at comparing LV function between standard and accelerated free-breathing sequences should focus on the population of patients with atrial fibrillation. Third, our accelerated cine sequence produced images with worse spatial and temporal resolution when compared to the traditional cine sequences. However, it is doubtful that this difference in resolution leads to significant clinically important differences. Fourth, while the initial evaluation of the novel accelerated cine sequence was conducted on patients referred for cardiomyopathy, a logical initial population to evaluate, it is important to subsequently evaluate its performance in a broad array of patient populations. Future studies should focus on its evaluation in diverse patient populations including those with congenital heart disease and cardiac masses. Fifth, we evaluated the novel accelerated sequence in a 1.5 T imaging environment exclusively. Off-resonance artifacts from the radial acquisition may be more pronounced at 3 T and future studies should focus on evaluating the sequence in the 3 T environment. Finally, although it is true that the traditional cine images were ranked slightly higher on a qualitative image quality scale, both sequences were in a similar range and there was no statistically significant difference between them with regard to this qualitative parameter. More importantly, our quantitative analyses showed that there were no significant differences in the calculation of key parameters of left ventricular structure and function, most notably LVEF, between the accelerated and traditional techniques.

5. Conclusions

The novel, accelerated free-breathing SSFP cine sequence that we evaluated performed similarly to standard of care multiple breath-hold cine SSFP and was acquired in a fraction of the time without the need for breath holding. If applied to clinical practice, these results lay the foundations for a significant potential reduction of scanning time and may also facilitate scanning in those patients who are unable to breath-hold.

Supplementary data to this article can be found online at https://doi.org/10.1016/j.mri.2019.06.008.

Funding sources

This research is supported by an operating grant from the Federal Development Agency of Canada and a matching financial contribution from HeartVista Inc. HeartVista Inc. provided a prototype version of their accelerated cine sequence for our evaluation. The funding bodies

had no role in the design of the study and collection, analysis and interpretation of data and in writing the manuscript.

References

[1] Achenbach S, Barkhausen J, Beer M, Beerbaum P, Dill T, et al. Consensus recommendations of the German Radiology Society (DRG), the German Cardiac Society (DGK) and the German Society for Pediatric Cardiology (DGPK) on the use of cardiac imaging with computed tomography and magnetic resonance imaging. Rofo 2012;184:345–68.

[2] American College of Cardiology Foundation Task Force on Expert Consensus D, Hundley WG, Bluemke DA, Finn JP, Flamm SD, et al. ACCF/ACR/AHA/NASCI/SCMR 2010 expert consensus document on cardiovascular magnetic resonance: a report of the American College of Cardiology Foundation Task Force on Expert Consensus Documents. J Am Coll Cardiol 2010;55:2614–62.

[3] Bellenger NG, Burgess MI, Ray SG, Lahiri A, Coats AJ, et al. Comparison of left ventricular ejection fraction and volumes in heart failure by echocardiography, radionuclide ventriculography and cardiovascular magnetic resonance; are they interchangeable? Eur Heart J 2000;21:1387–96.

[4] Bennett M, Parkash R, Nery P, Sénéchal M, Mondesert B, et al. CCS/CHRS 2016 Implantable Cardioverter-Defibrillator (ICD) Guidelines. Can J Cardiol.

[5] Maceira AM, Prasad SK, Khan M, Pennell DJ. Normalized left ventricular systolic and diastolic function by steady state free precession cardiovascular magnetic resonance. J Cardiovasc Magn Reson 2006;8:417–26.

[6] Scheffler K, Lehnhardt S. Principles and applications of balanced SSFP techniques. Eur Radiol 2003;13:2409–18.

[7] Suinesiaputra A, Bluemke DA, Cowan BR, Friedrich MG, Kramer CM, et al. Quantification of LV function and mass by cardiovascular magnetic resonance: multi-center variability and consensus contours. J Cardiovasc Magn Reson 2015;17:63.

[8] Grothues F, Smith GC, Moon JC, Bellenger NG, Collins P, et al. Comparison of interstudy reproducibility of cardiovascular magnetic resonance with two-dimensional echocardiography in normal subjects and in patients with heart failure or left ventricular hypertrophy. Am J Cardiol 2002;90:29–34.

[9] Emery DJ, Forster AJ, Shojania KG, Magnan S, Tubman M, et al. Management of MRI wait lists in Canada. Health Policy 2009;4:76–86.

[10] Roifman I, Paterson DI, Jimenez-Juan L, Friedrich MG, Howarth AG, et al. The state of cardiovascular magnetic resonance imaging in Canada: results from the CanSCMR pan-Canadian survey. Can J Cardiol 2018;34:333–6.

[11] Griswold MA, Jakob PM, Nittka M, Goldfarb JW, Haase A. Partially parallel imaging with localized sensitivities (PILS). Magn Reson Med 2000;44:602–9.

[12] Kido T, Kido T, Nakamura M, Watanabe K, Schmidt M, et al. Compressed sensing real-time cine cardiovascular magnetic resonance: accurate assessment of left ventricular function in a single-breath-hold. J Cardiovasc Magn Reson 2016;18:50.

[13] Schulz-Menger J, Bluemke DA, Bremerich J, Flamm SD, Fogel MA, et al. Standardized image interpretation and post processing in cardiovascular magnetic resonance: Society for Cardiovascular Magnetic Resonance (SCMR) board of trustees task force on standardized post processing. J Cardiovasc Magn Reson 2013;15:35.

[14] Roifman I, Paul GA, Zia MI, Williams LK, Watkins S, et al. The effect of percutaneous coronary intervention of chronically totally occluded coronary arteries on left ventricular global and regional systolic function. Can J Cardiol 2013;29:1436–42.

[15] Roifman I, Ghugre NR, Vira T, Zia MI, Zavodni A, et al. Assessment of the longitudinal changes in infarct heterogeneity post myocardial infarction. BMC Cardiovasc Disord 2016;16:198.

[16] Roifman I, Ghugre N, Zia MI, Farkouh ME, Zavodni A, et al. Diabetes is an independent predictor of right ventricular dysfunction post ST-elevation myocardial infarction. Cardiovasc Diabetol 2016;15:34.

[17] Roifman I, Zia MI, Zavodni A, Wolff R, Ghugre NR, et al. Evolution of right ventricular function post-acute ST elevation myocardial infarction. J Magn Reson Imaging 2014;40:709–14.

[18] Hunold P, Schlosser T, Vogt FM, Eggebrecht H, Schmermund A, et al. Myocardial late enhancement in contrast-enhanced cardiac MRI: distinction between infarction scar and non-infarction-related disease. AJR Am J Roentgenol 2005;184:1420–6.

[19] Bohl S, Wassmuth R, Abdel-Aty H, Rudolph A, Messroghli D, et al. Delayed enhancement cardiac magnetic resonance imaging reveals typical patterns of myocardial injury in patients with various forms of non-ischemic heart disease. Int J Cardiovasc Imaging 2008;24:597–607.

[20] White RD, Patel MR, Abbara S, Bluemke DA, Herfkens RJ, et al. 2013 ACCF/ACR/ASE/ASNC/SCCT/SCMR appropriate utilization of cardiovascular imaging in heart failure: an executive summary: a joint report of the ACR Appropriateness Criteria (R) Committee and the ACCF Appropriate Use Criteria Task Force. J Am Coll Radiol 2013;10:493–500.

[21] D'Andrea A, Fontana M, Cocchia R, Scarafile R, Calabro R, et al. Cardiovascular magnetic resonance in the evaluation of heart failure: a luxury or a need? J Cardiovasc Med (Hagerstown) 2012;13:24–31.

[22] Buechel EV, Kaiser T, Jackson C, Schmitz A, Kellenberger CJ. Normal right- and left ventricular volumes and myocardial mass in children measured by steady state free precession cardiovascular magnetic resonance. J Cardiovasc Magn Reson 2009;11:19.

[23] Semelka RC, Tomei E, Wagner S, Mayo J, Caputo G, et al. Interstudy reproducibility of dimensional and functional measurements between cine magnetic resonance studies in the morphologically abnormal left ventricle. Am Heart J 1990;119:1367–73.

[24] Semelka RC, Tomei E, Wagner S, Mayo J, Kondo C, et al. Normal left ventricular dimensions and function: interstudy reproducibility of measurements with cine MR imaging. Radiology 1990;174:763–8.

[25] Bottini PB, Carr AA, Prisant LM, Flickinger FW, Allison JD, et al. Magnetic resonance imaging compared to echocardiography to assess left ventricular mass in the hypertensive patient. Am J Hypertens 1995;8:221–8.

[26] Al-Khatib SM, Stevenson WG, Ackerman MJ, Bryant WJ, Callans DJ, et al. 2017 AHA/ACC/HRS Guideline for Management of Patients with Ventricular Arrhythmias and the Prevention of Sudden Cardiac Death: a Report of the American College of Cardiology/American Heart Association Task Force on Clinical Practice Guidelines and the Heart Rhythm Society. J Am Coll Cardiol 2018;72:e91–220.

[27] 2016 report on the health of Canadians; the burden of heart failure. Heart and Stroke Foundation of Canada; 2016.

[28] Goebel J, Nensa F, Bomas B, Schemuth HP, Maderwald S, et al. Real-time SPARSE-SENSE cardiac cine MR imaging: optimization of image reconstruction and sequence validation. Eur Radiol 2016;26:4482–9.

[29] Goebel J, Nensa F, Schemuth HP, Maderwald S, Quick HH, et al. Real-time SPARSE-SENSE cine MR imaging in atrial fibrillation: a feasibility study. Acta Radiol 2017;58:922–8.

[30] Xue H, Kellman P, Larocca G, Arai AE, Hansen MS. High spatial and temporal resolution retrospective cine cardiovascular magnetic resonance from shortened free breathing real-time acquisitions. J Cardiovasc Magn Reson 2013;15:102.

[31] Lin W, Huang F, Simonotto E, Duensing GR, Reykowski A. Off-resonance artifacts correction with convolution in k-space (ORACLE). Magn Reson Med 2012;67:1547–55.

[32] Connelly KA, Detsky JS, Graham JJ, Paul G, Vijayaragavan R, et al. Multicontrast late gadolinium enhancement imaging enables viability and wall motion assessment in a single acquisition with reduced scan times. J Magn Reson Imaging 2009;30:771–7.

[33] Voit D, Zhang S, Unterberg-Buchwald C, Sohns JM, Lotz J, et al. Real-time cardiovascular magnetic resonance at 1.5 T using balanced SSFP and 40 ms resolution. J Cardiovasc Magn Reson 2013;15:79.